A 2,3-Connected Tellurium Net and the Cs_3Te_{22} Phase

Qiang Liu, Norman Goldberg, and Roald Hoffmann*

Abstract: The bonding in the recently reported Cs_3Te_{22} phase, which contains both Te_8 rings and remarkable Te_6 sheets, is studied by approximate molecular orbital theory. Our focus is on the geometric and electronic features of the unique 2,3-connected Te net found as a substructure in this phase. The calculations show that both the linear and T-shaped Te geometries in the 2,3-connected Te net of Cs_3Te_{22} are determined by their particular electron count. Both types of tellurium atoms are hypervalent; we make connections to other well known hypervalent molecules, such as XeF_2, I_3^-, and BrF_3. Several possible variations and distortions of this net are discussed, all of which are found to be less stable. The discrete crown-shaped Te_8 units that appear in the phase show normal covalent bonding and should occur in smaller molecular entities, too. According to our computations, Cs_3Te_{22} should be metallic. Two structurally related phases, $CsTe_7$ and Cs_2Te_{15}, are suggested.

Keywords
band structures · hypervalent bonding · semiempirical calculations · tellurium compounds

Introduction

Over the past few years the chemistry of tellurium has blossomed. In both discrete molecules and extended systems tellurium has been found to display a wide range of unusual geometrical and bonding features.[1, 2]

An example of the richness of tellurium bonding[3] may be found in cesium tellurides. At least nine binary caesium telluride phases[4–11] ($CsTe_4$, $CsTe_5$, Cs_2Te, Cs_2Te_2, Cs_2Te_3, Cs_2Te_5, Cs_3Te_2, Cs_5Te_3, and Cs_5Te_4)[12] had been reported earlier. In many of these there is Te–Te bonding, but quite different in nature. For example, $CsTe_4$ contains isolated Te_8^{2-} chains, T-shaped, and four-coordinate Te atoms;[8] in Cs_2Te_5 there are one-dimensional $[Te_4Te_{2/2}]^{2-}$ chains containing both two- and four-coordinate Te atoms.[4]

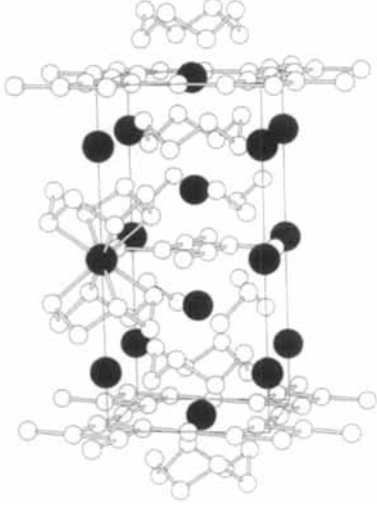

Fig. 1. The structure of Cs_3Te_{22}. One unit cell is outlined. Small circles represent Te atoms; Cs atoms are marked black. The few Te_2 groupings in the unit cell are actually truncated fragments of Te_8 rings.

Last year yet another binary phase (Cs_3Te_{22}) was reported.[13, 14] The beautiful structure of this compound (Fig. 1) displays a number of unusual features. Discrete crown Te_8 entities can be easily identified in Figure 1. Though such eight-membered crown-shaped molecules are well known for sulfur and selenium, they had not been previously observed for tellurium. Also apparent are infinite two-dimensional sheets that are formed by Te atoms and which include one Cs atom per six telluriums. The Cs atom in the $CsTe_6$ sheet, located in the center of a large square of twelve Te atoms, also lies at the center of an almost perfect cube, which is built from two sets of four Te atoms each belonging to a Te_8 crown (one such Te_8CsTe_8 unit is highlighted in Fig. 1). The structure may also be described as consisting of two different types of layers: $CsTe_6$ sheets separated by layers of $CsTe_8$ crowns.

Following Zintl's concept,[15] Cs_3Te_{22} can be written formally as $[Cs_3^{3+}][Te_{22}^{3-}]$. If one assumes the Te_8 rings to be neutral molecular entities and assigns the valence electrons of caesium fully to the tellurium sheets, the compound may be described as $[CsTe_8]_2^{2+}[CsTe_6]^{2-}$.

The pattern of the $CsTe_6$ sheet (Scheme 1) is interesting in that a C_4 axis is the principal symmetry element present (aside from twofold rotation axes and the mirror plane containing the sheet itself). The structure of this 2,3-connected sheet, constituted of linear and T-shaped tellurium atoms, belongs to the two-dimensional $P4$ space group (no. 10).

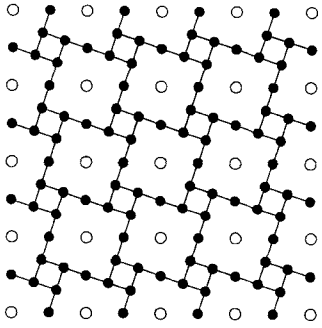

Scheme 1. Pattern of the $CsTe_6$ sheet looking down the c axis (open circles are Cs, filled circles Te).

Several aspects of this new binary compound are of interest: the geometrical and electronic nature of linear and T-shaped Te atoms in the $CsTe_6$ sheet; the electronic structure of the whole sheet, as unusual as it is; possible variants or distortions of this sheet; the stability of the crown Te_8; and possible conducting properties of this Cs_3Te_{22} phase. We address these questions below.

[*] R. Hoffmann, Q. Liu, N. Goldberg
Department of Chemistry and the Materials Science Center
Cornell University, Ithaca, NY 14853-1301 (USA)
Fax: Int. code +(607)255-5707

0947-6539/96/0204-0390 $ 15.00+.25/0

Results and Discussion

Linear Te in the $CsTe_6$ Sheet: There are two kinds of Te atoms in the $CsTe_6$ sheet. One is linear, bound to two other Te atoms. We will call this Te2. The other, which we call Te3, is T-shaped and bound to three Te atoms (Scheme 2). It is important to note here that the Te2 and Te3 notation does not refer to a crystallographic numbering; it is our way of reminding ourselves of the coordination environment of each Te. We start our analysis of the planar net by separately analyzing these building elements of the net, using molecular models.

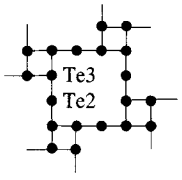

Scheme 2.

For two-coordinate main-group EX_2 molecules both bent (H_2O, H_2Se, H_2Te, and Te_3^{2-}) and linear configurations (XeF_2 and I_3^-) are possible. Why is Te2 linear in the sheet?

We begin by looking at a simplified model, H_2Te^{n-} using the extended Hückel (EH) method.[16] The H–Te distance is set at 1.69 Å.[17] Following the total energy while varying the H-Te-H bond angle, we find, not surprisingly, that the preferred geometrical configuration of H_2Te depends strongly on its electron count (or the total charge). The molecule prefers a bent geometry when it is neutral, as expected, and is linear for H_2Te^{2-}, analogous to a hypervalent H_2Xe or F_2Xe.

A more realistic model for the atomic environment of Te2 in the solid might be Te_3^{n-}. The Te–Te distance (3.077 Å) for which we carried out the calculations is taken from the Cs_3Te_{22} X-ray data. Again the computed structure depends strongly on the electron count. The linear configuration is favored for 3 –, 4 –, and 5 – charges.

Let us look at the Te_3^{4-} model more closely. The Walsh diagram[18] for the opening of the Te-Te-Te angle is depicted in Figure 2. On the left side (90°), both the highest occupied molecular orbital (HOMO) $4b_2$ and the lowest unoccupied molecular orbital (LUMO) $5a_1$ are slightly antibonding. As the angle increases from 90 to 180° the $5a_1$ becomes less antibonding, losing the p contribution from the central tellurium atom, and is stabilized significantly. On the other hand $4b_2$ is destabilized as the (antibonding) p–p σ overlap between the tellurium orbitals increases. The $4b_2$ and the $5a_1$ cross at approximately 110°. The rapid stabilization of the $5a_1$ (now the HOMO) as 180° is approached determines the preferred linear configuration for a Te_3^{4-} electron count.

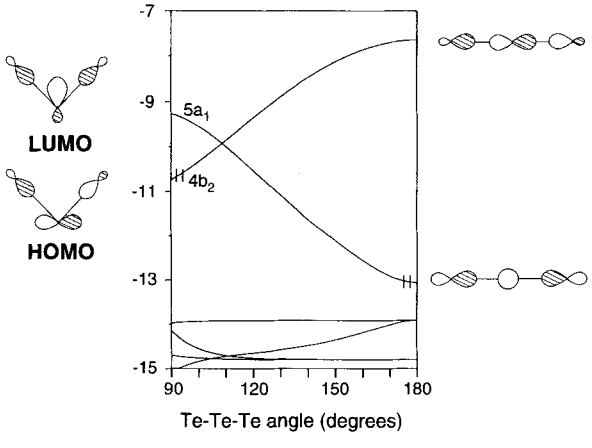

Fig. 2. Walsh diagram for the variation in bond angle in Te_3^{4-}.

A connection needs to be made here to the classical and well-characterized linear triiodide I_3^-. This species is, of course, isoelectronic to Te_3^{4-}, as is the related XeF_2. The bonding in I_3^- or XeF_2 is very well understood[17, 19, 20]—we have in these molecules an electron-rich three-center bond. If one omits the s orbital on the central atom from the bonding, one expects the level pattern shown on the left in Scheme 3, while if the s orbital is included, we get the pattern shown on the right. Note in either case that one and only one I-I-I antibonding orbital remains unfilled, $4b_2$ in Figure 2. The $5a_1$ and $4b_2$ orbitals of our Te_3^{4-} match, of course, the top two orbitals in Scheme 3 (right); counterparts of the other orbitals are also there in Figure 2, but are not specifically identified.

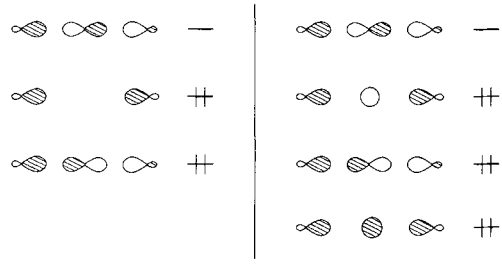
Scheme 3.

But what Te_3^{n-} charge makes for a good model for Te2 in the fourfold sheet of interest to us? As we shall see later, the approximate charge on Te2 in Cs_3Te_{22} is near to –1. Taking this computed charge seriously, and transferring it to the model at hand, this corresponds formally to $[H_2Te]^-$ and Te_3^{3-}. For these electron counts linear structures are energetically favored in the model compounds. What at first sight seems like a "normal" two-coordinate tellurium is actually a hypervalent atom, its geometry determined by the electron count. Indeed it does not make sense to think of a linear Te as being involved in normal bonding, for the preferred angle at the heavier Group VI elements in normal XEX compounds is close to 90°.

T-Shaped Te in the $CsTe_6$ Sheet: T-shaped subunits have been found in a number of tellurium compounds.[13] In this section, we will investigate the electronic reason for their appearance in the $CsTe_6$ sheet.

We use two discrete molecular units, $Te_4H_4^{n-}$ and $Te_4Te_4^{n-}$ (Scheme 4), as our models, based on the structural motif found in the sheet. The geometry of the small Te_4 square is taken from Cs_3Te_{22}, with a Te–Te bond length of 3.003 Å. Again X–Te distances of 1.69 Å for X = H and 3.077 Å for X = Te are used.

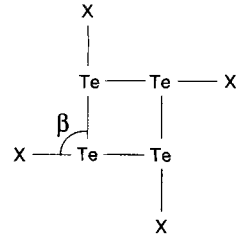

Scheme 4. X = H, Te.

Varying the X-Te-Te angle (β in Scheme 4) while maintaining fourfold symmetry, we calculate that the β = 90° configuration (C_{4h}) is more stable than the β = 135° (D_{4h}) conformer if the molecule possesses a total charge of –1 to –5 (X = H) or –5 to –9 (X = Te). In all the cases studied, the total energy actually minimizes at β < 90°. This might explain why the experimentally determined Te2-Te3-Te3 angle in the sheet is found to be 88.5 instead of 90°.[21]

Let's consider $[Te_4Te_4]^{n-}$ in some detail, and specify an 8 – total charge for the molecule, for reasons that will become clear below. A number of frontier orbitals (see the Walsh dia-

  0947-6539/96/0204-0391 $ 15.00+.25/0

gram, retaining a C_4 axis in Fig. 3) are involved in determining the structure of this molecule. Upon changing β from 90 to 135°, $6a_g$ is stabilized and turns into the LUMO (for that 8 − total charge), since the antibonding interaction between Te2 and Te3 in that orbital disappears. The doubly degenerate $6e_u$ does not change much. The $5b_g$ orbital (HOMO at 90°) is much stabilized, mainly owing to the decrease in overlap between orbitals on Te2 and Te3. The $5e_u$ orbital (doubly degenerate) goes up in energy only very little. The $5a_g$ orbital, which is slightly antibonding between Te2 and Te3, is greatly destabilized and ends up as a HOMO at 135°. As a result, the calculated HOMO–LUMO gap of about 6 eV at $\beta = 90°$ decreases to about 2 eV at $\beta = 135°$, and the $\beta = 135°$ configuration turns out to be considerably less stable. It is interesting to note that the stable configuration is *not* determined by the HOMO, but by levels below it, not all of which are shown in the energy window of Figure 3.

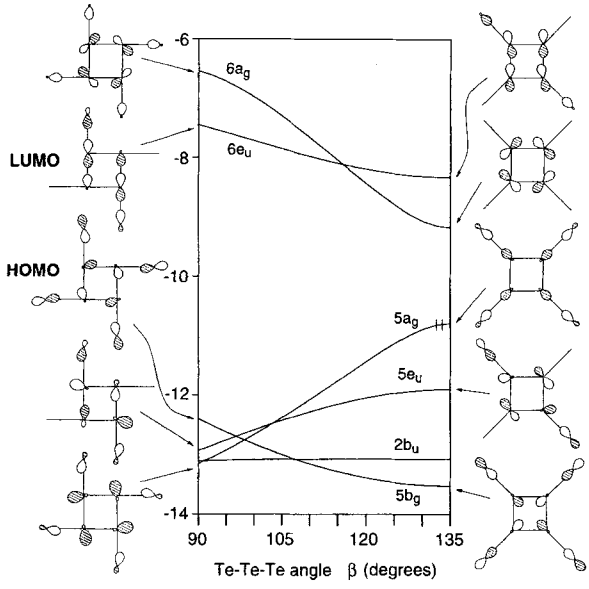

Fig. 3. Walsh diagram for the variation in the Te-Te-Te angle β of $[Te_4Te_4]^{8-}$ (see Scheme 4).

Can we see a reasonable electron count in some related molecule, the way we correlated Te_3^{4-} with I_3^- or XeF_2? There aren't that many square or fourfold symmetric molecules around. E_4^{2+} species (E = S, Se, Te) are known,[17] as is Bi_4^{2-},[22] and they are isoelectronic with the electronically happy $C_4H_4^{2-}$. To our knowledge there are no square hypervalent molecular groupings with halogens, noble gases, or metals. If we take E_4^{2+} and tetraprotonate the lone pairs pointing radially out of the E_4 ring, we get $E_4H_4^{6+}$, for which one would expect a classical D_{4h} structure ($\beta = 135°$). Clearly our Te_4 unit is much reduced relative to this hypothetical classical species. So hypervalent bonding, and the attendant T shape at Te is no surprise.

The T shape reminds one of the BrF_3 molecule, whose bonding is described qualitatively in Scheme 5 (left). Note the formal F^- nature of the "axial" fluorines. We see two lone pairs on the Br, a "normal" equatorial Br–F bond, and electron-rich three-center F-Br-F axial bonding. BrF_3 is clearly related to SF_4 and XeF_2. A tellurium analogue (Scheme 5, right) would be Te_4^{4-}.

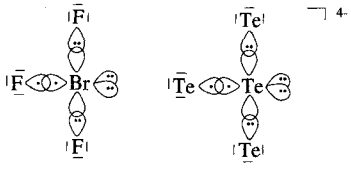

Scheme 5.

Can we set up an analogous bonding pattern in the tellurium square? It is not obvious how one should do this, for a given Te3–Te3 bond which is "axial" with respect to one Te3 and "equatorial" with respect to the other. But if we simply make all the bonds initially covalent and add two lone pairs at each Te, we get $[Te_4H_4]^{4-}$ or $[Te_4Te_4]^{8-}$ (Scheme 6). This is one extreme, and it is from this model that we derived the electron count used earlier.

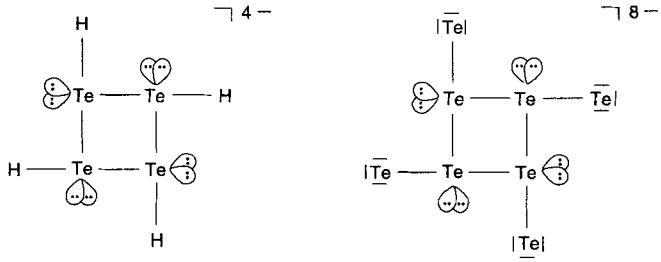

Scheme 6.

Now let's try an alternative approach to electron counting, beginning with the known solid-state structure. Formally, the sheet is $[CsTe_6]^{2-}$ or, assuming a Zintl viewpoint, Te_6^{3-}. We want to carve out, on paper, a Te_4 or Te_4Te_4 unit out of the solid. Assuming a covalent Te2–Te3 bond, breaking that bond homolytically, and keeping all the charges on the ring, we end up with the tetraradical Te_4^{3-}. Saturation of such radicals by H atoms leads to $[Te_4H_4]^{3-}$. Replacing those H atoms by isovalent Te^- anions, we arrive at a $[Te_4Te_4]^{7-}$ model.

A third approach to electron counting is simply to look at the charge distribution per Te_4 square calculated for the Te_6^{3-} or $[CsTe_6]^{2-}$ net. This calculation, discussed in the next section, leads to an approximate $(Te3)_4$ charge of −1. If we break (on paper) the Te2–Te3 bonds homolytically, and then "passivate" the dangling bonds by H or Te^-, we get to $[Te_4H_4]^-$ and $[Te_4Te_4]^{5-}$.

Returning now to our models, for all of these electron counts the $\beta = 90°$ configuration (or T-shaped Te3) is favored over large values of β. As in the case of the linear Te2 structure, the geometry of the T-shaped Te3 is also determined by electron count.

Let's look at the structure at hand in still another way. Each Te2 (linear) is hypervalent, and (if it were maximally hypervalent) could be assigned an electronic structure such as that shown in Scheme 7 (left) and a formal charge of −2. Each Te3 can be assigned a locally hypervalent structure (Scheme 7, right) and a −1 formal charge. With these charges throughout the net, we would have a charge per formula unit, $(Te3)_4(Te2)_2$, of −8. However, the actual charge is only −3! In other words, our Te_6^{3-} net is hypervalent (as the T-shaped Te3 and linear Te2 indicate), but it is not "maximally hypervalent", that is, it does not contain as many electrons as these hypervalent geometries would allow. It is this intermediate reduction stage that makes the electronic structure of Te_6^{3-} truly nonclassical and requires a delocalized bonding description.

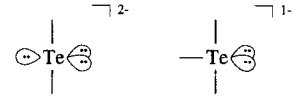

Scheme 7.

The reader might think these electron counting arguments tortuous. Indeed they are, but they are attempts to relate known molecular electron structures to this strange yet simple net. To give up trying is to give up understanding.

0947-6539/96/0204-0392 $ 15.00+.25/0 Chem. Eur. J. 1996, 2, No. 4

The $CsTe_6$ Sheet: We have analyzed the bonding in the structural subunits of the planar $[CsTe_6]^{2-}$ sheet and now consider the whole net. A calculation on the full $[CsTe_6]^{2-}$ net gives a +0.78 charge on Cs. Obviously a Zintl viewpoint, with nearly full electron transfer from Cs to the Te net, is reasonable. We thus turn our attention to a Te_6^{3-} net, whose band structure is shown in Figure 4.[23] Every point in our argument below was checked by calculations on $[CsTe_6]^{2-}$ as well; the analysis carries over, essentially unchanged.

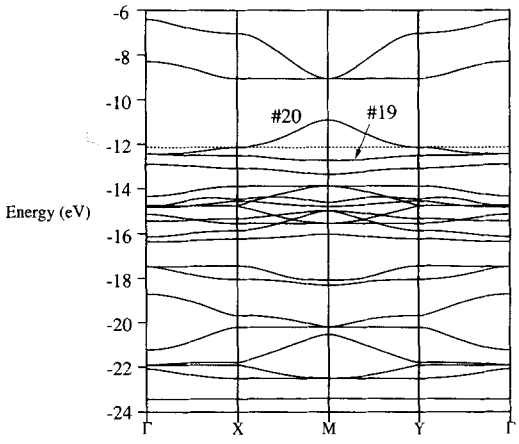

Fig. 4. Band structure of the Te_6^{3-} sheet. The dotted line indicates the Fermi level.

Most bands of the Te_6^{3-} net are quite flat, indicating weak interactions among Te atoms. This is a result of the relatively large Te–Te distances of 3.003 and 3.077 Å, as compared to 2.84 Å in elemental helical Te_x.[17] The band around the Fermi energy[24] is only half filled, since there is an odd number of valence electrons per Te_6^{3-} unit. Above that band we find a gap of about 2 eV.

Where are the electrons in this structure? We may partially answer the question and trace the nature of some bands by examining the contributions of individual atomic orbitals to the density of states (DOS).[25]

Most of the bonding in the valence region is accomplished by Te 5p orbitals. The in-plane locally π-type 5p orbitals (Scheme 8a) of Te2 form a narrow band between −16 and −14 eV; these orbitals are 98% below the Fermi energy. We do not show their contribution to the DOS. The contributions of the $5p_z$'s of the Te atoms (the z axis is normal to the plane formed by the sheet) to the DOS are displayed in Figure 5. For both Te2 and Te3, the p_z bands are relatively narrow; the π-type interactions between these orbitals are small. All contributions from these orbitals occur below the Fermi level; this indicates that these p_z's are filled with two electrons.

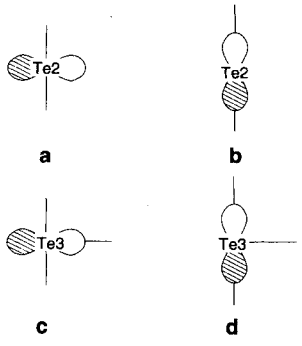

Scheme 8. Te2 and Te3 5p orbitals.

Figure 6 shows the contributions of the remaining 5p orbitals of Te2 and Te3 (Scheme 8b–d) to the DOS. The projected DOS's of the orbitals of Scheme 8b (on Te2) and 8d (on Te3) are surprisingly quite different. The former is less dispersed (probably a consequence of the slightly longer bond length),

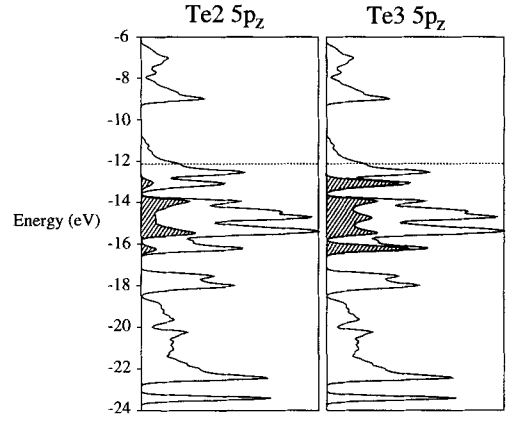

Fig. 5. Contributions (shaded areas) to the density of states (DOS) of the $5p_z$ orbitals on Te2 (left) and on Te3 (right). The solid curve is the total DOS for the Te_6^{3-} sheet. The Fermi energy is indicated by the dotted line.

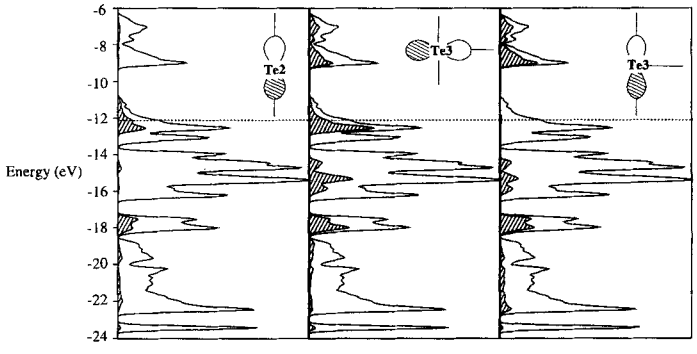

Fig. 6. Contributions (shaded areas) to the DOS of the various 5p orbitals shown in Scheme 8: b (left), c (middle), and d (right).

and is concentrated around −18 eV as well as the Fermi energy. The orbitals of the type shown in Scheme 8d contribute a lot to the states between −9 and −6 eV, but very few such levels are found around the Fermi energy. The orbital in Scheme 8c (on Te3), however, has significant contributions around the Fermi level.

To understand this, we go back to the Te_4Te_4 molecular model. In Figure 3 (left), both orbitals of the type shown in Scheme 8b (in the model the "Te2" is actually a terminal tellurium) and 8c (on Te3) appear in the $5b_g$ (HOMO), $5e_u$, and $5a_g$ orbitals (and thus contribute to the DOS around the Fermi energy). The corresponding molecular orbitals in the sheet are bands no. 19 and 20 (numbered from the lowest energy band up, Fig. 4). Band no. 20 crosses the Fermi level around X. The crystal orbitals at Γ and M in these two bands are sketched in Scheme 9. Note the degeneracy of these bands at Γ. We see no

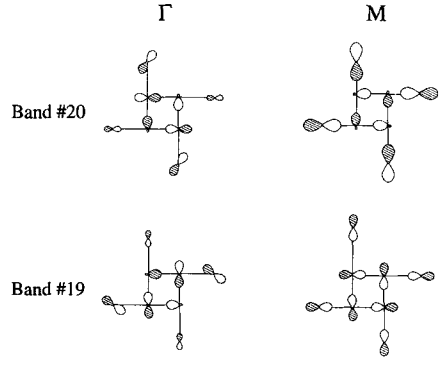

Scheme 9.

contributions from the orbitals of the type shown in Scheme 8d. Small mixing of 5s' into 5p's can be seen; this is responsible for the increase in energy of band no. 20 at M. Note furthermore that interactions between Te2–Te3 and Te3–Te3 are slightly antibonding or nonbonding in $5b_g$ and in bands no. 19 and 20.

The occupation of some Te–Te antibonding orbitals in the Te_6^{3-} sheet can be easily discerned from a crystal orbital overlap population (COOP)[25] analysis. At lower energies the states of the net are both Te2–Te3 and Te3–Te3 bonding (Fig. 7), while the states near the Fermi level are antibonding. Note that there are more antibonding orbitals filled for Te2–Te3; this should lead to a smaller average overlap population (OP).[26] Indeed the calculated average OP's are 0.17 for Te2–Te3 and 0.30 for Te3–Te3.

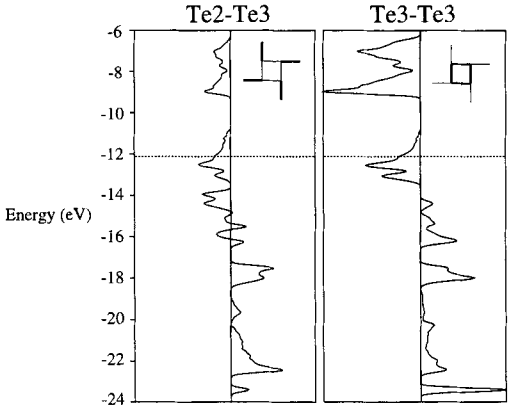

Fig. 7. Crystal orbital overlap population (COOP) for Te2–Te3 (left) and Te3–Te3 (right) bonding in the Te_6^{3-} sheet. Both COOP's are on the same scale. The Fermi energy is indicated by the dotted line.

To put these overlap populations into perspective, we compare them with OP's of four reference systems in Figure 8. Analogous to oxygen (O_2), Te_2 possesses a formal double bond between the two Te atoms. The models Te_2^{2-} and Te_3^{2-} are formally only singly bonded, and the three-center electron-rich Te_3^{4-} possesses a formal half bond. The Te2–Te3 and Te3–Te3 bonds in Te_6^{3-} (the same values are computed in $[CsTe_6]^{2-}$) are weak, with a bond order between 1/2 and 1.

Filling antibonding orbitals should also result in a lengthening of a bond, as observed for the Te–Te distances in the sheet. This can also be seen in the OP curves of Figure 8.

The Mulliken atomic charges[26] for the Te_6^{3-} sheet are −0.217 on Te3 and −1.065 on Te2. Since the Te_6^{3-} net contains four Te3 and two Te2 atoms per unit cell, we are led to

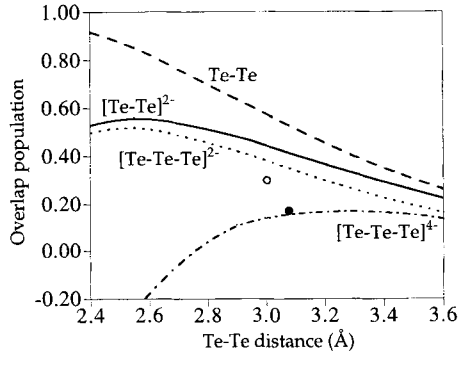

Fig. 8. Overlap population (OP) vs. distance for four reference systems. OP's are shown for Te2–Te3 (•) and Te3–Te3 (○), as calculated in the Te_6^{3-} net.

$[(Te3)_4]^{-0.87}$ and $[(Te2)_2]^{-2.13}$. This gives us another way to guess at the electron counts in the model we calculated earlier, the triatomic model for Te2 and the Te_4Te_4 square for Te3.

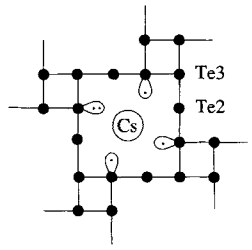

Scheme 10.

What are the consequences of an electron density of ≈6.25 on Te3? Consider Scheme 10. If we were to assume three covalent bonds and a p_z lone pair at Te3, we have 1.25 electrons on average to put into the Te3 lobe (part of orbital in Scheme 8c) that points toward the Cs atom. One could think of one such lobe filled with two electrons and three with one electron; then one would think of four such resonance structures permuting the two-electron atoms around the 12-membered ring. If instead of adopting such a simple model, we look at the actual orbital populations in the net, we find that the orbital shown in Scheme 8c is occupied on the average by 1.40 electrons. There are also lone pairs on Te2 pointing toward the Cs; these are not shown here. Clearly there is radical character in the Te_6 plane. In the solid state, the bandwidths arising from interactions between partially occupied orbitals may result in a low-spin state (or a half-filled band). But the possibility of a magnetic state should not be dismissed, based in part on this perceived radical character.

The negatively charged Te_6^{3-} net is stabilized by Cs^+ cations, both within the $[CsTe_6]^{2-}$ sheet and in the other layers of the Cs_3Te_{22} phase. Our simple MO treatment yields an energy difference of 0.67 eV between Te_6^{3-} and $[CsTe_6]^{2-}$, with the latter being more stable. Calculations including explicitly Madelung energy terms should give even more stabilization to $[CsTe_6]^{2-}$.

In summary, the electronic and geometrical structure of the $CsTe_6$ sheet is highly unusual. The bonds among Te atoms are weak and all tellurium atoms in the net are hypervalent.

Some Variations on the 2,3-Connected Net: The 2,3-connected Te_6 net (sheet) can be approximately derived from the 4-connected perfect square Te net (Scheme 11) by removing two-fifths of the Te squares (the open circles in Scheme 11). This neglects the 0.074 Å bond length difference and the 1.5° deviation of one Te-Te-Te angle from 90°. Alternatively, one arrives at the pure tellurium square net by substituting the Cs atom in $CsTe_6$ by a Te_4 unit.

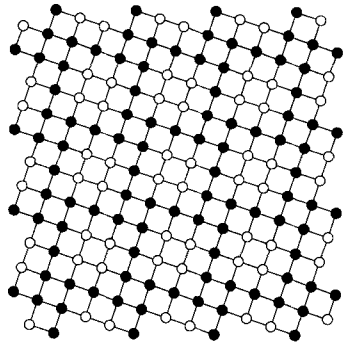

Scheme 11. 2,3-Connected Te_6 net derived from the 4-connected perfect square Te net.

Would such a square tellurium net be stable? Let's compare it with a Te_6^{3-} model. To make the comparison meaningful, we assign the same number of electrons to every Te atom; that is, each tellurium bears a formal charge of −0.5, as in the Te_6^{3-} net. This is not the charge distribution computed, but here just an expedient formalism. Furthermore the Te_6^{3-} net described in the previous sections is idealized, with all bond lengths set to 3.003 Å and angles taken as 90 and 180°.

The band structure for the square net is very simple, composed of only four bands.[25] The calculated energy per tellurium atom (actually $Te^{-0.5}$) in the square Te net is found to be

0947-6539/96/0204-0394 $ 15.00+.25/0 Chem. Eur. J. 1996, 2, No. 4

1.70 eV higher than that for tellurium atoms in the Te_6^{3-} net.[27] Thus, the square net is indeed much less stable than the experimentally observed "defect structure", in which some atoms are missing from a perfect square net. The reasons for the specific geometry assumed by the defect structure have been analyzed in the framework of a general study of such structures by Lee and Foran.[28]

It should be mentioned that perfect square nets of Te have been reported to exist as sublattices in lanthanide tellurides of the type $LnTe_n$ ($2 \leq n \leq 3$).[3, 29] In these compounds the square Te net carries a formal charge from -0.5 to -1. The Te···Te distance in the more highly reduced material is expanded; Böttcher[3] reasoned that this would be consistent with the antibonding nature of the additional occupied orbitals. Indeed we find this region of COOP for the square net Te–Te antibonding. However, the semiconductivity reported for these phases has raised serious doubt about the structural assignment.[30] As found recently, these compounds do in fact possess an as yet unknown superstructure.[31]

The 2,3-connected Te_6 net can also be viewed as a distortion from the more symmetrical net shown in Scheme 12. This net belongs to the plane group $P4mm$ (no. 11; we will call it a D_{4h} net since its unit cell is of this symmetry). By rotating the small Te_4 squares in this structure, the experimentally observed Te_6 sheet can be generated. Yet, the experimental structure constitutes again the more stable configuration, according to our calculations. The energy increases monotonically upon rotating the small squares in the experimentally observed Te_6^{3-} net to generate the D_{4h} net. The difference in energy between the two structures is computed to be 3.30 eV per Te_6 unit for $[CsTe_6]^{2-}$ and 2.688 eV for Te_6^{3-}. These are similar results to what we obtained for the Te_4Te_4 model in previous sections.

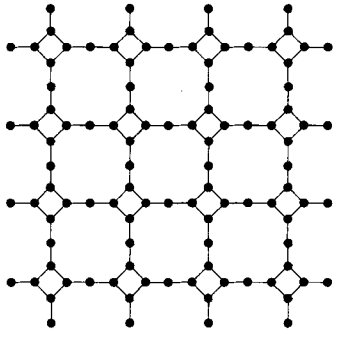

Scheme 12. Symmetrical net that can be related to the 2,3-connected Te_6 net.

The band structure of this hypothetical D_{4h} Te_6^{3-} sheet is shown in Figure 9 (experimental Te–Te bond lengths used). It resembles slightly the band structure calculated for the experimentally observed sheet (Fig. 4). However, the band gap which occurred around -10 eV in Figure 4 has disappeared here. One more band which was higher in energy in the experimental structure is lowered and moved into the window at about -7 eV. The two bands immediately below the Fermi energy at Γ in Figure 4 are raised by more than 1 eV, as is the Fermi energy. This is equivalent to a destabilization of $5e_u$ and $5a_g$ in the case of the molecular models (Fig. 3), and explains why the hypothetical sheet is less stable. One may also say that the D_{4h} structure is destabilized due to the fact that several bands in this structure have moved towards the Fermi energy instead of away from it. Or to put it another way, a two-dimensional Peierls-like distortion stabilizes the less symmetrical structure.

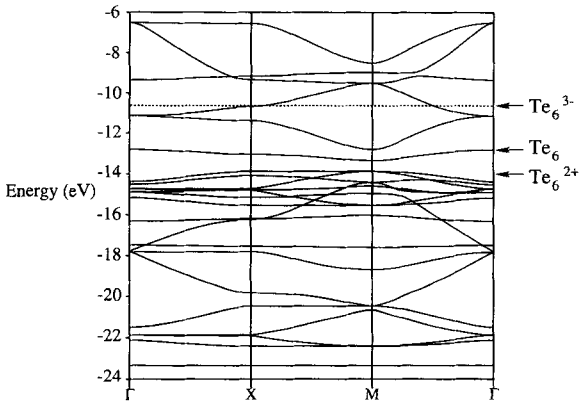

Fig. 9. Band structure for the hypothetical D_{4h} Te_6 sheet ($\beta = 135°$). The dotted line marks the Fermi level for the D_{4h} Te_6^{3-} net. Note the gaps that occur at two other marked electron counts.

The instability of the D_{4h} structure does not persist for all electron counts. In Figure 9 one sees that the D_{4h} net has small gaps at two places, for Te_6 and Te_6^{2+} electron counts. Indeed calculations for both these electron counts predict that the D_{4h} net is more stable than the Te_6^{3-} net by ≈ 0.5 eV.

Returning to the observed structure, a referee has suggested that it might be worthwhile to consider distortions of the net to "isolate" certain Te_n^{x-} substructures, perhaps in a way that one sees in polyiodide chains. Here are some of the more symmetrical partitionings that come to mind (see Scheme 13); each is illustrated as a substructure and can be thought of as propagating through the whole two-dimensional net. We do not trust the extended Hückel method to calculate the energetics of these distortions, especially in the absence of the caesiums. However, it is interesting to consider the electron counting possibilities of each. In Scheme 13a the partitioning generates four angular Te_3 units. The charge that each would have classically is Te_3^{2-} or -4 per Te_6 unit, which is in excess of the electrons available. In Scheme 13b one would have large Te_{12} rings. Each "angular" Te would be formally neutral; each linear Te would have a -2 charge. This would then lead to Te_{12}^{16-} or Te_6^{8-}, again too reduced. In Scheme 13c one gets Te_4 rings and isolated Te^{2-} ions. The Te_4 ring could be neutral (or $+2$, if one wants a Hückel π system in the ring). This then leads to a -4 charge per Te_6 (if the ring is neutral) or -2 (if the ring is charged $+2$). Scheme 13a and c are closer than Scheme 13b to the observed electronic content of the net.

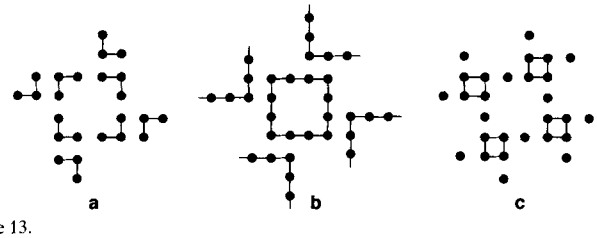

Scheme 13.

The Crown-Shaped Te_8 Unit and the Cs_3Te_{22} Phase: The experimentally observed crown-shaped Te_8 unit is only of C_4 symmetry, instead of the ideal D_{4d}. But the deviation is very small. Two factors are possibly responsible: the fact that the crystal only has a fourfold axis and the different environments of the two faces of the Te_8 crown.

Figure 10 (left) shows the energy-level diagram for a molecular crown Te_8 unit (geometry taken from Cs_3Te_{22}). Not surprisingly, a HOMO–LUMO gap of about 6 eV is found; this indicates that the Te_8 configuration is rather stable. The addition of a Cs^+ cation to the Te_8 unit (to formally give a $[Cs(\eta^4\text{-}1,3,5,7\text{-cyclo-}Te_8)]^+$ cation) lowers the total energy by 1.43 eV. Thus, the Te_8 rings in Cs_3Te_{22} are stabilized significantly by the Cs^+ cation.

The crown Te_8 molecule should exist as a discrete molecule and in complexes containing the M(η^4-1,3,5,7-cyclo-Te_8) group, where M could be a Cs^+ cation or some other transition metal ML_n fragment.

The projected DOS for Te_8 in the complete Cs_3Te_{22} structure is also shown in Figure 10 (right). The bands are dispersed a little as a result of small interactions with the Te_6 sheet; still the

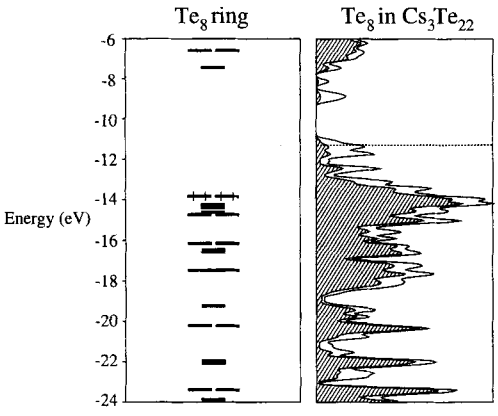

Fig. 10. Energy-level diagram (left) for the crown-shaped Te_8 molecule and contributions to the DOS of the Te_8 units (right) in Cs_3Te_{22}. All the levels below the HOMO (filling by electrons indicated) are occupied. The solid curve (right) indicates the total DOS for Cs_3Te_{22}.

energy level pattern for the Te_8 unit (shaded area, right panel) is readily recognizable. The interaction that is observed between Te subunits is probably caused by two relatively close contacts at 3.424 and 3.444 Å between tellurium atoms of the Te_8 ring and the Te_6 sheet. The most interesting consequence of this interaction is a small contribution of the Te_8 units to the DOS around the Fermi energy.

The changes in the DOS of the Te_6 sheet upon going to the three-dimensional structure are more pronounced. The large peaks around -15 eV (Fig. 5), which originated mainly from the $5p_z$'s of Te2 and Te3, have disappeared (Fig. 11, shaded areas; z is normal to the sheet plane and parallel to the c axis). It is those $5p_z$'s that interact mostly with the crown Te_8 ring and become more dispersed (Fig. 11, right). The gap at -10 eV, the DOS right above and below the Fermi energy, and the location of the Fermi energy itself are nevertheless mainly determined by the Te_6 sheet.

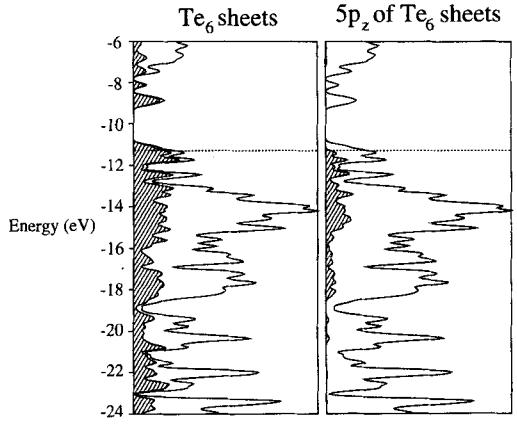

Fig. 11. Contributions (shaded areas) to the DOS of the Te_6 sheets in Cs_3Te_{22} (left) and of all the $5p_z$ orbitals of the telluriums in the sheets (right).

Each Te_6 sheet is one electron short of filling the band below the gap. Since there are two Te_6 unit in the unit cell, two more electrons are needed to fully occupy the bands below the gap in Cs_3Te_{22}. Owing to this half-filled band the Cs_3Te_{22} phase should be metallic.

However, there is another possibility. We mentioned before that the Te3's in the $CsTe_6$ sheet have radical lobes pointing toward the Cs atom. A group of four such lobes occupied by five electrons around a Cs is fairly isolated from other groups (though each interacting with a neighboring Te2 5p lone pair), and interaction among lobes within any such group is probably not very strong, either. This situation, shown schematically in Scheme 14 (left) for one Te2–Te3 group of four pointing toward a Cs, is reminiscent of a classical stable radical system, the nitroxyls (Scheme 14, right). This feature should persist on going from the sheet to the whole Cs_3Te_{22} phase. Thus the Cs_3Te_{22} phase might show some interesting magnetic properties.

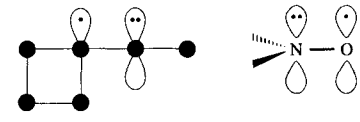

Scheme 14.

We calculate Mulliken charges of -0.82 on Te2, -0.16 on Te3, $+0.77$ on Cs (in the sheet), $+0.72$ on Cs (in Te_8 layers), and almost zero on the Te atoms which form the Te_8 rings. These charges are quite similar to those computed for $[CsTe_6]^{2-}$ and $[CsTe_8]^+$, and justify the application of the Zintl concept to this Cs_3Te_{22} phase. The OP's of 0.17 for Te2–Te3 and 0.30 for Te3–Te3 are the same as those calculated for $[CsTe_6]^{2-}$. The average OP's between Cs and Te atoms are almost zero, a sign of the mainly ionic bonding between them.

Summary

The crown-shaped Te_8 unit in the Cs_3Te_{22} phase is found to be a stable molecular entity which is further stabilized by the Cs^+ cations. There is some interaction between the Te_8 ring and the Te_6 sheet, but a reasonable approximation is to regard them as nearly separate entities. The electronic structure of the phase is mainly determined by the Te_6^{3-} sheet. The Cs_3Te_{22} phase is predicted to be conducting or magnetic.

Considering the nature of the layered structure of the Cs_3Te_{22} phase and the character of the bonding in the solid prompts us to suggest two other possible phases: $[CsTe_6]^-[CsTe_8]^+$, or $CsTe_7$ and $[CsTe_6]^{3-}[CsTe_8]_3^{3+}$, or Cs_2Te_{15}. Both should have structures similar to that of Cs_3Te_{22}, but composed of layers of $CsTe_6$ sheets and $CsTe_8$ units in 1:1 and 1:3 ratios, respectively. The $CsTe_7$ phase should again be metallic. Cs_2Te_{15} should be a semiconductor, however. Alternatively, a Cs_5Te_{22} structure, should there be room for two Cs atoms in the structure, should be semiconducting.

Appendix

Table 1 shows the extended Hückel parameters used in our calculations. For H, Cs, and Te, values are taken from earlier work [16,32,33]. Calculations were done using Greg Landrum's wonderful YAeHMOP (V1.0) program, available on the WWW at: http://overlap.chem.cornell.edu:8080/ yaehmop.html. The CACAO program [34] was used to visualize some of the orbitals. In computing average properties, the same 36 k-point set was used for the experimental Te_6^{3-} net, the D_{4h} structure, and the perfect square net. An 8 k-point set was chosen for the Cs_3Te_{22} calculation [35].

Acknowledgment: Special thanks are due to Greg Landrum for helpful remarks and suggestions on this manuscript. N. G. wishes to thank the Deutsche Forschungsge-

Table 1. Parameters used in extended Hückel calculations.

Atom	Orbital	H_{ii} (eV)	ζ_{i1}
H	1s	−13.60	1.30
Cs	6s	−3.88	1.06
	6p	−2.49	1.06
Te	5s	−20.80	2.51
	5p	−14.80	2.16

meinschaft (DFG) for the award of a research stipend which made his stay at the Cornell University possible. We are grateful to the National Science Foundation for supporting this work through Research Grant CHE-9408455, and through the NSF-MRL program under Award number DMR-9121654 to the Materials Science Center at Cornell.

Received: August 10, 1995 [F188]

[1] M. A. Ansari; J. M. McConnachie; J. A. Ibers, *Acc. Chem. Res.* **1993**, *26*, 574.
[2] J. Beck, *Angew. Chem. Int. Ed. Engl.* **1994**, *33*, 163.
[3] P. Böttcher, *Angew. Chem. Int. Ed. Engl.* **1988**, *27*, 759.
[4] P. Böttcher, U. Kretschmann, *Z. Anorg. Allg. Chem.* **1982**, *491*, 39.
[5] K. A. Chuntonov, A. N. Kuznetsov, V. M. Fedorov, S. P. Yatsenko, *Inorg. Mater.* **1982**, *18*, 937.
[6] K. A. Chuntonov, A. N. Orlov, S. P. Yatsenko, Y. N. Grin', L. D. Miroshnikova, *Inorg. Mater.* **1982**, *18*, 941.
[7] G. Prins, E. H. P. Cordfunke, *J. Less-Common Met.* **1984**, *104*, L1.
[8] P. Böttcher, U. Kretschmann, *Z. Anorg. Allg. Chem.* **1985**, *523*, 145.
[9] J. W. Hobbs, R. J. Pulham, *J. Chem. Res. Synop.* **1994**, 68.
[10] J. W. Hobbs, R. J. Pulham, *J. Chem. Res. Synop.* **1994**, 156.
[11] I. Schewe-Miller, P. Böttcher, *Z. Krist.* **1991**, *196*, 137.
[12] As a referee has pointed out to us, the characterisation of Cs_5Te_4 and $CsTe_5$ reported by Chuntonov et al. (Refs. [5] and [6]) is somewhat questionable, as attempts to verify this work by Prins and Cordfunke (Ref. [7]) have not been succesful.
[13] W. S. Sheldrick, M. Wachhold, *Angew. Chem. Int. Ed. Engl.* **1995**, *34*, 450.
[14] M. G. Kanatzidis, *Angew. Chem. Int. Ed. Engl.* **1995**, *34*, 2109.
[15] E. Zintl, *Angew. Chem.* **1939**, *1*, 52.
[16] R. Hoffmann, *J. Chem. Phys.* **1963**, *39*, 1397.
[17] N. N. Greenwood, A. Earnshaw, *Chemistry of the Elements*, Pergamon, New York, **1984**.
[18] A. D. Walsh, *J. Chem. Soc.* **1953**, 2260.
[19] B. M. Gimarc, *Molecular Structure and Bonding*, Academic Press, New York, **1979**.
[20] T. A. Albright, J. K. Burdett, M.-H. Whangbo, *Orbital Interactions in Chemistry*, John Wiley, New York, **1985**.
[21] What happens if we move the four terminal Te atoms in Te_4Te_4 out of the plane defined by the small Te_4 square? For the $\beta = 90°$ configuration bearing charges from −5 to −9, this deformation raises the total energy drastically. This argues for planarity (no out-of-plane puckering) of the $CsTe_6$ sheet.
[22] A. Cisar, J. D. Corbett, *Inorg. Chem.* **1977**, *16*, 2482.
[23] The structure of the $CsTe_6$ sheet belongs to the two-dimensional *P*4 space group (no. 10). Although its reciprocal lattice is the square Bravais lattice, its Brillouin Zone (BZ) only has C_4 symmetry, the sole symmetry element present in the sheet. Thus, its irreducible wedge is one quarter of the first BZ, instead of the usual one-eighth for a square lattice. For reference, see: S. L. Altmann, *Band Theory of Solids: an Introduction from the Point of View of Symmetry*, Clarendon, Oxford, **1991**.
[24] N. W. Ashcroft, N. D. Mermin, *Solid State Physics*, Holt, Rinehart & Winston, New York, **1976**.
[25] R. Hoffmann, *Solids and Surfaces: a Chemist's View of Bonding in Extended Structures*, VCH, New York, **1988**.
[26] R. S. Mulliken, *J. Chem. Phys.* **1955**, *23*, 1833; 1841; 2338; 2343.
[27] For comparison, a unit cell content of Te_{10}^{5-} was used in calculating the perfect square net.
[28] S. Lee, B. Foran, *J. Am. Chem. Soc.*, submitted.
[29] B. K. Norling, H. Steinfink, *Inorg. Chem.* **1966**, *5*, 1488.
[30] F. Hulliger, *Structural Chemistry of Layer-Type Phases*, Reidel, Dordrecht Holland, **1976** pp 242 ff.
[31] X. Zhang, J. Li, B. Foran, S. Lee, H.-Y. Guo, T. Hogan, C. R. Kannewurf, M. G. Kanatzidis, *J. Am. Chem. Soc.* **1995**, *117*, 10513.
[32] S. Alvarez, F. Mota, J. Novoa, *J. Am. Chem. Soc.* **1987**, *109*, 6586.
[33] M.-H. Whangbo, P. Gressier, *Inorg. Chem.* **1984**, *23*, 1228.
[34] C. Mealli, D. M. Proserpio, *J. Chem. Ed.* **1990**, *67*, 3399.
[35] R. Ramirez, M. C. Bohm, *Int. J. Quantum Chem.* **1988**, *34*, 571.